Atmos. Chem. Phys. Discuss., 9, 22739–22771, 2009
www.atmos-chem-phys-discuss.net/9/22739/2009/

Atmospheric Chemistry and Physics Discussions

This discussion paper is/has been under review for the journal *Atmospheric Chemistry and Physics (ACP)*. Please refer to the corresponding final paper in *ACP* if available.

Particle characterization at the Cape Verde atmospheric observatory during the 2007 RHaMBLe intensive

K. Müller, S. Lehmann, D. van Pinxteren, T. Gnauk, N. Niedermeier, A. Wiedensohler, and H. Herrmann

Leibniz-Institut für Troposphärenforschung e.V., Permoserstr. 15, 04318 Leipzig, Germany

Received: 9 September 2009 – Accepted: 15 September 2009 – Published: 27 October 2009

Correspondence to: H. Herrmann (herrmann@tropos.de)

Published by Copernicus Publications on behalf of the European Geosciences Union.

Abstract

The chemical characterization of filter high volume (HV) and Berner impactor (BI) samples PM during RHaMBLe 2007 shows that the Cape Verde aerosol particles are mainly composed of sea salt, mineral dust and associated water. The influence from the African continent on the aerosol constitution was generally small but air masses which came from south-western Europe crossing the Canary Islands transported dust to the sampling site together with other loadings. The mean mass concentration was determined for PM_{10} as 17 $\mu g/m^3$ from the impactor samples and as 24.2 $\mu g/m^3$ from HV filter samples. Non sea salt (nss) components of PM were found in the submicron fractions including nitrate in the coarse mode fraction. Bromide was found in all samples with much depleted concentrations in the range 1–8 ng/m^3 compared to fresh sea salt aerosol indicating intense atmospheric halogen chemistry. A chloride deficit of 31% and 38% for the coarse mode particles (3.5–10 μm; 1.2–3.5 μm), of 67% (0.42–1.2 μm) and 83% (0.14–0.42 μm) for the submicron fractions was determined.

During 14 May with high mineral dust loads also the maximum of OC (1.71 $\mu g/m^3$) and EC (1.25 $\mu g/m^3$) was measured. The minimum of TC (0.25 $\mu g/m^3$) was detected during the period 25 to 27 May when pure marine air masses arrived. The concentrations of carbonaceous material decrease with increasing particles size from 60% for the ultra fine particles to 2.5% in coarse mode PM.

Total iron (dust vs. non-dust: 0.53 vs. 0.06 $\mu g\,m^{-3}$), calcium (0.22 vs. 0.03 $\mu g\,m^{-3}$) and potassium (0.33 vs. 0.02 $\mu g\,m^{-3}$) were found as good indicators for dust periods because of their heavily increased concentration in the 1.2 to 3.5 μm fraction as compared to their concentration during the non-dust periods. For the organic constituents, oxalate (78–151 ng/m^3) and methanesulfonic acid (MSA, 25–100 ng/m^3) are the major compounds identified. A good correlation between nss-sulphate and MSA was found for the majority of days indicating active DMS chemistry and low anthropogenic influences.

1 Introduction

To investigate the influence of Saharan dust on the chemical processes in the atmosphere and the ocean, as well as the interaction between these two compartments, a detailed chemical characterization of the dust particles is necessary. The Sahara desert is well known as the world largest natural source of atmospheric dust (Heintzenberg, 2009; Washington et al., 2003). The dust emission and the atmospheric transport of dust are important sources of the iron nutrient for the subtropical and tropical North Atlantic Ocean and also for the Amazon basin (Martin, 1990). In turn, oceanic emissions influence atmospheric properties, e.g. cloud formation (Charlson et al., 1987; Kettle and Andreae, 2000). The interaction between the atmosphere and the surface layer of the ocean is an object of research for a while now. To better study the influence of dust on the ocean and the ocean's influence on the atmosphere, the construction of the atmospheric observatory at the Cape Verde isle (CVAO) São Vicente started in 2006. UK SOLAS, the German ministry for education and research (BMBF), the Leibniz-Institutes IfM-GEOMAR (Kiel) and IfT (Leipzig), the EU funded project TENATSO as well as the German Max-Planck-Society are the major founders of this research activity in close collaboration with the Cape Verde Instituto Nacional de Meteorologia e Geofísica (INMG) in the northern tropical Atlantic Ocean. Using the CVAO research site the chemical and physical characterization of PM (particulate matter) near the surface will be carried out for several years to identify the transport of Saharan dust into the Atlantic Ocean and to support the model verification by long-term data from a region heavily influenced by Saharan dust deposition.

São Vicente is already far enough from the source region and about 900 km in the main wind direction off the coast of West Africa (Mauretania and West Sahara). During the transportation of dust, chemical transformations can occur that can lead to a much greater solubility of iron than in the Saharan source regions (Baker and Jickells, 2006). There is an ongoing scientific discussion about iron solubility from emitted and processed mineral dust. The solubility of anthropogenic and natural aerosol iron was

determined in a wide variability between 0.01 and 80% (Spokes and Jickells, 1996; Baker et al., 2006; Solmon et al., 2009) and appears to be strongly dependent on acidity (Zhu et al., 1992; Manicelli et al., 2005). Furthermore, organic ligands, like oxalate in aerosols or siderophores in seawater, do enhance the solubility of iron significantly (Kraemer, 2004).

Besides the quasi-continuous filter sampling, during RHaMBLE (Lee et al., 2009), in an intensive measurement campaign the present work focused on the investigation of size-resolved marine particulates in five size fractions with respect to the analysis of mass, concentration of ionic components, organic and elemental carbon (OC; EC), iron, and organic single compounds (MSA and dicarboxylic acids) as well as number concentration and size distribution. Such data sets have been often requested (e.g., Mahowald et al., 2005) but only a few data are actually existing from source regions but not from the main deposition region in the tropical North Atlantic with the exception of the work of Chiapello et al. (1995). These authors collected filter samples over three years for metal analyses at the Cape Verde island Sal. From some ship cruises in this region also short time aerosol particle data exist (e.g., Chen and Siefert, 2004; Rijkenberg et al., 2008).

For future modeling, long term experimental data about the total dust deposition and its size-resolved chemical composition are needed.

2 Experimental

2.1 Site description and sampling

The Cape Verde Islands are a volcanic archipelago 700 km off the west coast of Africa. The Cape Verde Atmospheric Observatory (CVAO – Observatório Atmospherico de Cabo Verde: Humberto Duarte Fonseca) was built in 2006 on the north-east coast of the island of São Vicente (16°51′50″ N, 24°52′2″ W, 10 m a.s.l.), 70 m from the coastline. Prevailing north-eastern trade winds heading from the Canary Islands and the

ACPD
9, 22739–22771, 2009

North African continent are blowing directly off the ocean. On the coast, influences from the island itself like dispersed dust, orographic influences in dust sedimentation or anthropogenic emissions are small in the area. The climate on São Vicente is arid with a maximum of 50 mm rainfall per year. Therefore dominantly dry dust deposition is to be expected. The annual average temperature is about 25°C. For the aerosol measurements a 30 m high tower was built to reduce the strong influence of the sea spray on the samples (inlet height: 32 m).

The particle sampling for the RHaMBLe intensive took place between 14 May 2007 and 14 June 2007. Filter and impactor samples have been taken in a 24-hour-mode in general. From 25 May to 8 June the mode was changed to 48-h due to extremely clean air masses and non-detectable amounts of PM in the size-resolved samples.

A high volume Digitel filter sampler DHA-80 (Walter Riemer Messtechnik, Germany) with PM_{10}-inlet was installed on top of the 30 m high tower. Samples were collected on annealed 150 mm quartz fiber filters (Munktell, MK 360) with an average flow rate of 500 l/min. For the size-resolved impactor samples a 5-stage Berner impactor (Hauke, Gmunden, Austria) made of stainless steel was also mounted in 30 m height. It was operated with a flow rate of 75 l/min. As the substrate material annealed aluminum foils were used. Additional Nuclepore foils (Wicom, Heppenheim, Germany) for the determination of metals were exposed on each stage (stage 1: 0.05–0.14 μm, stage 2: 0.14–0.42 μm, stage 3: 0.42–1.2 μm, stage 4: 1.2–3.5 µm, stage 5: 3.5–10 µm). A PM_{10} isokinetic inlet was mounted on the impactor.

After sampling all filters and aluminum foils were stored in aluminum boxes at 5°C at the station. The Nuclepore-foils were stored in polystyrene boxes. To avoid transport disturbances all samples were transported as hand luggage under ambient conditions to Leipzig. The filters and aluminum foils were equilibrated for 3 d at 20°C and 50% relative humidity. Masses were determined by the use of micro-balances (HV-filter: Mettler AT261 Delta Range, impactor foils: Mettler Toledo UMT2). For further chemical analysis the filters have been divided into quarters, the aluminum foils were divided by the number of particle spots, differing between size fractions (38–53% for ion analysis,

25–40% for OC/EC analysis 7–10% for metal analysis and 8–28 % for organic single species analysis).

2.2 Analytical methods

Ion analysis

For ion analysis Digitel filters were extracted with 30 ml MilliQ-water (15 min shaker, 15 min ultrasonic bath, 15 min shaker), Berner samples with 2 ml MilliQ-water (10 min shaker, 10 min ultrasonic bath, 10 min shaker). All samples were prefiltered with 0.45 μm one-way syringe filters to remove insoluble materials. Ion analysis was performed for cations Na^+, NH_4^+, K^+, Mg^{2+}, Ca^{2+} with ion-chromatography (IC) (Waters IC-Pak C M/D Column, eluent: 0.1 mM EDTA, 3.0 mM HNO_3). To determine bromide along the high chloride-concentrations of the sea salt, a special column Metrosep A Supp 5 (Metrohm) was used in a Compact IC 761 (Metrohm LTD, Switzerland) to measure the anions Cl^-, Br^-, NO_3^-, SO_4^{2-} and $C_2O_4^{2-}$ (eluent: 1 mM $NaHCO_3$/3.2 mM Na_2CO_3, flow rate: 0,7 ml/min).

Methanesulfonic acid (MSA) was analyzed from the filtrated aqueous extract using capillary electrophoresis (CE) with indirect UV detection. The Spectra Phoresis 1000 (Thermo Separation Products, USA) was equipped with a fused silica capillary (70 cm length, 63 cm to detector, 75 µm i.d.). For separation, the capillary was filled with a background electrolyte consisting of 10 mmol l^{-1} p-aminobenzoic acid, 8 mmol l^{-1} diethylenetriamine, and 3.5 mmol l^{-1} aqueous sodium hydroxide (pH=9.6). After hydrodynamic injection at 10.3 kPa for 30 s, a separation voltage of 30 kV was applied. Indirect detection was performed at 254 nm.

Metal analysis

In a cold oxygen plasma the Nuclepore®-foils were ashed within 1.5 h. Metal analysis for total Ca, Fe, Zn, Mn and K was performed with Total Reflection X-Ray Fluorescence

Spectrometer (TXRF) S2 Picofox (Bruker AXS, Berlin, Germany) on the polished quartz substrates for the size segregated samples of the Berner impactor using a Mo-X-ray source. Gallium was used as an internal standard. Depending on the size fraction different concentrations were applied (10 ng for the three submicrometer fractions and 100 ng for the coarse mode fraction).

OC/EC analysis

OC/EC was determined for all filter and impactor samples by a two step thermographic method using a carbon analyzer C-mat 5500 (Ströhlein, Germany) published in Herrmann et al. (2006). The estimation of organic matter (OM) was performed following Turpin et al. (2000) using the equation OM=2∗OC, which is recommended for aged aerosols.

Physical PM characterization

To obtain the particle number size distribution in the range of 0.01 to 10 μm, a SMPS (Scanning Mobility Particle Sizer) in combination with an APS (Aerodynamic Particle Sizer, TSI 3321, TSI Inc., St. Paul Minnesota, USA) were used. The SMPS consists of a DMA (Differential Mobility Analyzer, type Hauke medium) with a selected particle size range of 0.01 to 0.9 µm in combination with a CPC (Condensation Particle Counter, TSI 3010, TSI Inc., St. Paul Minnesota, USA). The fundamentals of the SMPS technique are explained in Birmili et al. (1999), who described the instruments and working routine of a T-DMPS (Twin-Differential Mobility Particle Sizer). There are some differences between the SMPS and T-DMPS. The SMPS has a closed loop system, in which the DMA sheath air is re-circulated. The relative humidity for the closed loop varies between 20 and 40%. To get a better time resolution, the voltage setting in the DMA is not stepping (T-DMPS) but scanning (SMPS). With the APS, particle number size distributions in the size range between 0.6 and 10 μm (aerodynamic diameter) are obtained. To combine the particle number size distributions of the SMPS and the APS,

the aerodynamic particle diameters of the APS were converted to volume equivalent diameters (DeCarlo et al., 2004) which is the same diameter as used for the SMPS. The used overlap diameters (0.7–0.9 μm) between the SMPS and the APS distributions were averaged to combine both distributions. The inlet of the measurement system was installed only 4 m above ground on the top of the measurement container.

3 Results and discussion

3.1 Back trajectory investigation

For the interpretation of the size-fractionated PM constitution the history of the air mass is more important than the local meteorological conditions because the high atmospheric life time of submicron particles. Using the NOAA HYSPLIT (HYbrid Single-Particle Lagrangian Integrated Trajectory) model the back trajectories were calculated for each day (starting 500 m above ground). In Fig. 1a back trajectories (72 h) between 8 and 13 May are summarized to show the air mass origin over north-western Africa. As can be seen from this figure, before the campaign started (14 May), a Saharan dust event (daily mean dust concentration on 10/11 May: 332 μg/m^3) took place over São Vicente. Figure 1b summarizes the back trajectories (72 h) during the intensive measurement period (14 May to 14 June, Julian days 133 to 164). From the back trajectories and the mass determination analysis, only two major classes of samples may be distinguished: (i) continental (dust and anthropogenical emissions) and (ii) only marine aerosol. Only during the beginning of measurements an influence of the African continent was observed by wearing off the Saharan dust event between 8 and 13 May (Fig. 1a). A weak continental influence was found for air masses from southwestern Europe and the Canary Islands. All other air masses have their origin in the Atlantic, North and Northwest of Cape Verde.

3.2 PM characterization

Mass concentration of PM was investigated using three different methods, i.e. impactors, HV-filter sampler and SMPS-APS method. Impactor sampling allows mass determination and chemical characterization of the five size fractions. Filter sampling delivers a high total mass for the chemical analyses and the SMPS-APS measurements provide number concentration in 100 size channels within a high time resolution. It has to be noted that a direct comparison for the measurements described here between the offline sampling methods and the physical SMPS-APS measurements is not possible as the inlets of the samplers deployed were not operated at the same height level of the measurement tower, cf. Sect. 3 and Fig. 8.

Impactor measurements

For the impactor sampling, 23 samples in five size fractions each (15 daily and 8 two-day samples) were analyzed. Deduced from the total PM concentration only two samples showed mineral dust influence, i.e., summed up to PM_{10}: 14–15 May: 69.0 $\mu g/m^3$ and 15–16 May: 39.4 $\mu g/m^3$ because of their high mass concentration. All other samples were predominantly of maritime origin. Mass concentrations of the single stages summed up to PM_{10} are presented in Fig. 2. Mass concentration varied between 12 and 24 $\mu g/m^3$ with a mean of 17 $\mu g/m^3$ for these maritime aerosols.

In Fig. 3, the mean size distributions of the detected PM constituents are shown for the days influenced by mineral dust (a) and (b) for the maritime days. The water content of PM is not considered. The estimation of the mineral dust content is made only from the iron content according to the mean of 4% in Saharan dust.

The three size classes below 1.2 μm show elevated mass concentrations resulting from secondary aerosol formation from marine and anthropogenic sources and mineral dust during a number of days. All these air masses came across SW Europe and the Canary Islands. The detailed distribution is shown in Fig. 4 for important PM constituents between particle size fractions.

BI stage 1 (Dp=0.05–0.14 μm) and BI stage 2 (0.14–0.42 μm)

In contrast to the constitution of continental aerosol an extremely low concentration of ultra fine particles (0.05–0.14 μm) was found in all samples. In the two smallest size fractions the mass concentrations were below 0.2 $\mu g/m^3$ for 0.05–0.14 μm and up to 1.7 $\mu g/m^3$ in the 0.14–0.42 μm fraction and consisted mostly of OC and nss components. Low concentrations of elemental carbon from this PM long range transported were observed. Ammonium and nss-sulphate are the major ions. The observed chloride deficit of 83 and 67% is in good agreement with size-resolved measurements by Keene et al. (2004). Less dominant other anions in these fractions are nitrate, oxalate, and methanesulfonate. Potassium, magnesium, and calcium were found as minor cations. Considering the ion balance and the water content a mean pH-value of 0.5 was estimated for the 0.14–0.42 μm fraction which is in good agreement with the estimation of Herrmann (2003).

BI stage 3 (Dp=0.42–1.2 μm)

In comparison to continental aerosols where the most abundant PM-fraction is observed between 0.42–1.2 μm, the mass-dominating PM-fractions at the CVAO were observed between 1.2–10 μm. In the 0.42–1.2 μm fraction, externally mixed sea salt, mineral dust and long range transported secondary PM were found, leading to the differences in the observed pattern in comparison to typical continental aerosols. Dust day samples and non-dust day samples are not distinguishably in this fraction by mass, only by minor constituents, e.g. trace metals iron and calcium. The chloride deficit if found to 83±14% in this size range.

Due to the similarities in the size distribution between sea salt and Saharan dust with their maximum in the super-micron range the differences in mass between dust and marine influenced aerosol could not be observed. However, the concentration of calcium, potassium and iron (Table 1) were used as an indication for dust influence.

BI stage 4 (Dp=1.2–3.5 μm) and BI stage 5 (Dp=3.5–10 μm)

The PM concentration maximum was detected in the size fraction 1.2–3.5 μm (8.70 µg/m^3) followed by the coarse mode fraction 3.5–10 μm (7.33 µg/m^3). The super-micron fractions were dominated by sodium, chloride, calcium, potassium and magnesium from sea salt but during dust days calcium and potassium were found in higher fraction than in sea salt and mineral dust is the main constituent. The high concentration of nitrate in coarse mode particles originates from the reaction of gaseous nitric acid with sea salt sodium chloride. A chloride deficit of 31±10% for the fraction 3.5–10 μm and 38±10% for the fraction 1.2–3.5 μm was detected. These effects of HNO_3 in polluted air masses on the particle composition at the Cape Verdes during RHaMBLe are being discussed by Lawler et al. (2009) in line with the findings of the present study.

As a minor component bromide was detected with the maximum concentration typically found at BI stage 4. The observed bromide deficit at both coarse mode fractions of 89±8% is very high and in line with a very active photochemical halogen activation chemistry leading to considerable amounts of BrO in the gas phase as being identified for the first time for non-polar regions by Read et al. (2008a). Similar high deficits were reported by Ayers et al. (1999) from Cape Grim summer measurements and by Gabriel et al. (2002) from the Indian Ocean.

The findings of the size distribution and mean concentrations in the samples influenced by dust compared to the marine samples are summarized in Fig. 4 for selected PM constituents.

Organic particle phase constituents

For organic single species, only oxalate, malonate, succinate and MSA were detected. A few measurements found sugars (glucose, arabitol and mannitol) in concentrations below 3.4 ng/m^3. Mean concentration of dicarboxylic acids and MSA are presented in Table 2. For MSA the mean concentration was determined to 30 ng/m^3. During the

ACPD
9, 22739–22771, 2009

dust event the maximum was measured to 67 ng/m^3. The distribution of MSA between size fractions yield a maximum in the 0.42–1.2 and 1.2–3.5 μm size classes. These findings and the size distribution are in good agreement with data from Johansen et al. (2000) from a ship cruise near Cape Verde. Organic tracers of anthropogenic origin, e.g. PAH, were not found in this study. Surprisingly, in the Cape Verde aerosol particles a number of organic amines has been identified as well as some simple sugars. These findings are being discussed separately by Müller et al. (2009).

Metals

The particle total metal content was only analyzed from Berner impactor samples using TXRF. Total calcium, potassium and iron concentrations and their ratios to the total stage mass collected are summarized in Table 1. From all samples the size fraction below 3.5 µm was analyzed. The PM on Nuclepore-foils of stage 5 (3.5–10 µm) were not visible at all samples rendering the analysis for higher dust concentrations impossible because the TXRF needs a piece of sample smaller than 9 mm in diameter with a distinct PM deposition spot. Hence, a total of 13 samples of BI stage 5 could not be analyzed. A direct comparison between high and low dust concentrations in the fraction between 3.5 and 10 μm is hardly possible. Stage 3 and 4 (0.42–1.2–3.5 µm) are the most interesting fractions for the mineral dust determination, given that the highest total mass concentration was also found on stage 4. The high concentrations of Fe, Ca and K during the dust event compared to their concentrations during low dust days confirm their role as mineral dust indicators.

Calcium concentrations increased during high dust days (9 times higher than during low dust) due to mineral fractions of the source areas. Moreno et al. (2006) reported calcite as an important mineral in the Western Sahara. There is good agreement for the calcium concentrations measured by IC for the water soluble part and by TXRF for total calcium (r^2=0.99). Only 6% of calcium is found in non-soluble material (Fig. 5).

During 14 and 15 May, backward trajectories indicate a preferential direction from

Western Africa and Canary Islands. The concentration of iron in the Saharan dust was about 4 wt% (e.g., Moreno et al., 2006; Schroth et al., 2009). The total iron concentration in the high dust sample during the RHaMBLe intensive was 1.7 wt%. Our findings with respect to the sea salt, organic matter and water content of the collected PM are in good agreement with the values of Schroth et al. (2009). For the estimation of mineral dust in our samples (compare Fig. 3) the iron concentration (4% of dust) was used as the basis.

Chemical mass closure for the impactor measurements

An aerosol mass closure for PM deposited on the impactor stages is possible by the estimation of total mineral dust and the water content. The water content was determined by the ionic constitution after Neusüß et al. (2000) and the r.H. of 50% at weighing. In the different size fractions the amount of water was found between 5% for the nano-particles to 47% in the marine coarse mode PM. Taking into account the estimation for water and dust for the sum of the impactor stages gives 95±10% for the mass closure. However, in the nano-particle stage a higher error was determined due to analytical and weighing uncertainties to a value of 98±51%. The water soluble ions, mainly sea salt, contribute to 56±9% to the total mass during non-dusty times. In the two dusty samples the ionic contribution was only 31, resp. 44%. The sum of OM and EC contribute to the total PM_{10} mass between 1.6 and 9%. During non-dusty days, the contribution of mineral dust was estimated to 0.7 to 7.9% to the total mass collected, in dusty samples to 30%. Compared to the monthly mean concentrations of 2007, May and June occur as expected as low-dust summer months, where most of the dust from the African continent is transported in higher atmospheric layers above Cape Verde Islands (Prospero and Carlson, 1981; Chiapello et al., 1995; Schepanski et al., 2009). The dust contribution to the total aerosol during RHaMBLe intensive is in good agreement with the monthly mean of 4 $\mu g/m^3$ for May and June reported for the years 1992–1994 by Chiapello et al. (1995) for the island Sal.

Filter measurements

More than 90 $\mu g/m^3$ of PM_{10} were detected in 31 samples during these two years, 22 in winter, four in spring and fall each, and one in summer. For May 2007, an exceptional high dust event was observed at São Vicente (PM_{10} mass concentration during 10 to 11 May: 332 $\mu g/m^3$) but this peak of dust was wearing with the start of the intensive measurements. With the exception of the first two samples (92 and 50 $\mu g/m^3$) the detected mass concentration of PM_{10} particles was low (15–31 $\mu g/m^3$). Figure 6 shows the monthly mean PM_{10} concentration and the monthly maximum of our filter sampling data. The observations of Chiapello et al. (1995) about the Saharan dust concentrations were confirmed at the CVAO at São Vicente during HV-filter sampling in the years 2007 and 2008.

Ionic constituents contribute with 43 to 65% to the mass. The aerosol bromide concentration (1–8 ng/m^3) observed is much lower than expected from sea salt, compared to sodium concentration in PM. The water content of the filter samples was calculated between 27 and 48%. OM and EC were generally found between 1.5 and 6% of the total mass.

The methanesulfonic acid concentration and the detected nss-sulphate indicate an active DMS chemistry above the tropical Atlantic (Fig. 7) where not only OH but also Cl appears to be involved, cf. Lawler et al. (2009). Results for MSA are in good agreement with the data reported by Yang et al. (2009) from the North Yellow Sea and Allan et al. (2009) from the RRS Discovery during 25 and 26 May when the Discovery was close to Cape Verde. Earlier measurements of MSA and nss-sulphate showed no correlation to DMS (Read et al., 2008b).

The chemical mass closure for the HV-filter samples is hardly possible because the uncertainties at the water content and the mineral dust fraction which was not measured from filter samples.

SMPS-APS measurements

The physical PM characterization delivered number concentration size distribution with high time resolution. Characteristic daily variations were not observed for the number concentration as well as for the size distribution.

In Fig. 7, two particle number size distributions are shown. The first one (filled squares) was measured at 15 May within the last days of the dust event that occurred between 9 May and 15 May. A typical bimodal distribution for marine air is seen for particles smaller than 0.5 μm with the maxima at 0.045 and 0.2 μm. Particles of these modes mainly consist of nss-sulfate, carbonaceous species and a few smaller sea salt particles. Also, a dominant mode with the maximum at 0.5 μm is visible for this first distribution including the dust particles from the Saharan desert. Particle diameters >10 μm were not measured but cannot be excluded.

The second distribution (open squares) was measured 4 d after the dust event and is mainly influenced by the oceanic emissions and secondary formed PM. In the submicron range until 0.5 μm a difference to the first distribution was observed. The number concentration at 0.06 and 0.13 μm was higher than during the dust event. For the second distribution, a third flat mode at 0.5 μm is also visible but with a much lower number concentration and the largest particles are smaller than 6 μm.

Comparison of techniques in use

The differences between the HV-filter- and the impactor-measurements were observed previously and have different causes (Wieprecht et al., 2004). The inlet cutoff of the filter sampler, the higher adsorption of gaseous compounds and the higher water uptake by the quartz fiber filters are possible causes as well as the volatility of NH_4NO_3 and other semivolatile components in the low pressure impactor. In Fig. 9 the mass concentration differences between sampling systems are shown.

During this campaign, the inlet for the physical measurements was mounted just 4 m above ground, so that all measurements are influenced by the very strong sea spray

that occurs close to the coast line. This is also the reason for the mass differences between chemical and physical measurements since the chemical measurements were conducted on top of the 30 m tower and were therefore hardly affected by the sea spray. The determination of masses from physical measurements was carried out with an aerosol density of 2.1 g/cm^3 which is an estimate for dry sea salt.

The PM_{10} bromide concentration was found much lower than expected from the sea salt concentration. According to this observation, intense chemical bromine activation must be the cause for the bromide loss in PM. A good agreement between filter and impactor samples was found. The small difference between both methods can be explained by uncertainties of the analytical method near the detection limit. Pszenny and Keene (personal communication) measured total bromine by Neutron Activation Analysis (NAA) using a TSP sampler and found all the time 2–4 times higher bromine concentrations than our ion chromatographic method. Both methods have not been compared before. The different sampling systems and the determination of non-ionic bromine by NAA may cause the differences (Fig. 10).

4 Summary and conclusions

Within the present study two different sampling systems for PM and physical characterization for number and size distribution were applied during the RHaMBLe intensive campaign. With the exception of the first two days where a Saharan dust event came to its end, mainly marine aerosols were measured at the CVAO. The mean mass concentration of the marine PM_{10} aerosol was about 24 μg/m^3 at filters and 17 μg/m^3 in impactor samples. Sea salt, water, long range transported dust and secondary aerosol components were found in varying proportion according to the PM size fraction. Minimal continental and anthropogenic influences have been observed by their EC content and mineral dust traces (iron and calcium) in air masses coming from southwestern Europe and the Canary Islands. The size segregated chemical aerosol characterization has found a high percentage of carbonaceous material in the Aitken mode particles

decreasing with size increase. From the physical number size distribution, concentration peaks at 0.045 and 0.2 μm during the marine air mass origin indicate a weak anthropogenic influence. Size fractions 0.14–0.42 and 0.42–1.2 μm were dominated by secondary ionic material, long range transported dust and OC/EC. The coarse mode PM fractions are dominated by sea salt and water and during the first days by mineral dust. In the size-resolved impactor and the filter samples typical values of the chloride deficit were detected. In sub-micrometer PM the loss can reach 100% decreasing with increasing particle size to 31%. For the bromide PM content, a high deficit of 89% from the coarse mode impactor fractions and of 88% was found from the PM10 filter samples. Both deficits for the particle phase halogenide ions point to an active halogene activation photochemistry. Finally, particle phase MSA indicates an active DMS oxidation chemistry.

Acknowledgement. The IfT participation at the CVAO is supported by the German BMBF SOPRAN project (FKZ 03F0462J). Additional support through the EC project TENATSO (Project No.37090) and the WGL SAW project TRACES is acknowledged. The authors do thank Bruno Faria and Luis Mendes for their substantial help at the CVAO on São Vicente and the CVAO. We thank B. Keene and A. Pszenny for helpful discussions and providing the NAA Bromine data. Thanks also to Katie Read for the DMS data and their help at the CVAO. We acknowledge the laboratory work of A.Thomas, E. Neumann, A. Dietze, and B. Gerlach.

References

Allan, J. D., Topping, D. O., Good, N., Irwin, M., Flynn, M., Williams, P. I., Coe, H., Baker, A. R., Martino, M., Niedermeier, N., Wiedensohler, A., Lehmann, S., Müller, K., Herrmann, H., and McFiggans, G.: Composition and properties of atmospheric particles in the eastern Atlantic and impacts on gas phase uptake rates, Atmos. Chem. Phys. Discuss., 9, 18331–18374, 2009, http://www.atmos-chem-phys-discuss.net/9/18331/2009/.

Ayers, G. R., Gillett, R. W., Cainey, J. M., and Dick, A. L.: Chloride and bromide loss from sea-salt particles in southern ocean air, J. Atmos. Chem., 33, 299–319, 1999.

Baker, A. R., French, M., and Linge, K. L.: Trends in aerosol nutrient solubility along a west-east transect of the Saharan dust plume, Geophys. Res. Lett., 33, L07805, doi:10.2005GL024764, 2006.

Baker, A. R. and Jickells, T. D.: Mineral particle size as a control on aerosol iron solubility, Geophys. Res. Lett., 33, L17608, doi:10.1029/2006GL026557, 2006.

Birmili, W., Stratmann, F., and Wiedensohler, A.: Design of a DMA-based size spectrometer for a large particle size range and stable operation, J. Aerosol Sci., 30, 549–553, 1999.

Charlson, R. J., Lovelock, J. E., Andreae, M. O., and Warren, S. G.: Oceanic phytoplankton, atmospheric sulphur, cloud albedo and climate, Nature, 326, 655–661, 1987.

Chen, Y. and Siefert, R. L.: Seasonal and spatial distribution s and dry deposition fluxes of atmospheric total and labile iron over the tropical and subtropical North Atlantic Ocean, J. Geophys. Res., 109, D09305, doi:10.1029/2003JD003958, 2004.

Chiapello, I., Bergametti, G., Gomes, L., Chatenet, B., Dulac, F., Pimenta, J., and Santos Suares, E.: An additional low layer transport of sahelian and saharan dust over the north-eastern tropical Atlantic, Geophys. Res. Lett., 22, 3191–3194, 1995.

DeCarlo, P. F., Slowik, J. G., Warsnop, D. R., Davidovits, P., and Jimenez, J. L.: Particle morphology and density characterization by combined mobility and aerodynamic diameter measurements. Part 1: Theory, Aerosol Sci. Technol., 38, 1185–1205, 2004.

Gabriel, R., von Glasow, R., Sander, R., Andreae, M. O., and Crutzen, P. J.: Bromide content of sea-salt aerosol particles collected over the Indian Ocean during INDOEX 1999, J. Geophys. Res., 107(D19), 8032, doi:10.1029/2001JD001133, 2002.

Heintzenberg, J.: The SAMUM-1 experiment over Southern Morocco: overview and introduction, Tellus, 61B, 2–11, 2009.

Herrmann, H.: Kinetics of aqueous phase reactions relevant for atmospheric chemistry, Chem. Rev., 103, 4691–4716, 2003.

Herrmann, H., Brüggemann, E., Franck, U., Gnauk, T., Löschau, G., Müller, K., Plewka, A., and Spindler, G.: A source study of PM in saxony by size-segregated characterization, J. Atmos. Chem., 55, 103–130, 2006.

Johansen, A. M., Siefert, R. L., and Hoffmann, M. R.: Chemical composition of aerosol collected over the tropical North Atlantic Ocean, J. Geophys. Res., 105, 15277–15312, 2000.

Keene, W. C., Pszenny, A. A. P., Maben, J. R., Stevenson, E., and Wall, A.: Closure evaluation of size-resolved aerosol pH in the New England coastal atmosphere during summer, J. Geophys. Res., 109, D23307, doi:10.1029/2004JD004801, 2004.

Kettle, A. J. and Andreae, M. O.: Flux of dimethylsulfide from the oceans: a comparison of updated data sets and flux models, J. Geophys. Res., 105, 26793–26808, 2000.

Kraemer, S. M.: Iron oxide dissolution and solubility in the presence of siderophores, Aquat. Sci., 66, 3–18, 2004.

Lawler, M. J., Finley, B. D., Keene, W. C., Pszenny, A. A. P., Read, K. A., von Glasow, R., and Saltzmann, E. S.: Pollution-enhanced reactive chlorine chemistry in the eastern tropical Atlantic boundary layer, Geophys. Res. Lett., 36, L08810, doi:10.1029/2008GL036666, 2009.

Lee, J. D., McFiggans, G., Allan, J. D., Carpenter, L. J., Jones, C. E., Lewis, A. C., Moller, S. J., Read, K. A., Methven, J., Fuentes, E., Good, N., Irwin, M., Commane, R., Furneaux, K. L., Goddard, A., Ingham, T., Whalley, L. K., Heard, D. E., Mahajan, A., Oetjen, H., Plane, J. M. C., Saiz-Lopez, A., Hollingsworth, A., Ball, S. M., Benton, A., Jones, R., Baker, A. R., O'Doherty, S., Young, D., Müller, K., Lehmann, S., Niedermeier, N., Müller, T., Herrmann, H., Wiedensohler, A., Pszenny, A. A. P., Keene, W. C., Long, M. S., Sander, R., Lawler, M. J., Saltzman, E. S., and Finley, B. D.: Reactive Halogens in the Marine Boundary Layer (RHaMBLe): context of the tropical North Atlantic Ocean experiments, Atmos. Chem. Phys. Discuss., in press, 2009.

Lim, H.-J., Turpin, B. J., Russel, L. M., and Bates, T. S.: Organic and elemental carbon measured during ACE-Asia suggests a longer atmospheric lifetime, Environ. Sci. Technol., 37, 3055–3061, 2003.

Mahowald, N. M., Baker, A. R., Bergametti, G., Brooks, N., Duce, R. A., Jickells, T. D., Kubilay, N., Prospero, J. M., and Tegen, I.: Atmospheric global dust cycle and iron inputs to the ocean, Global Biogeochem. Cy., 19, GB4025, doi:10.1029/2004GB002402, 2005.

Manicelli, V., Decesari, S., Facchini, M. C., Fuzzi, S., and Mangani, F.: Partitioning of metals between the aqueous phase and suspended insoluble material in fog droplets, Ann. Chim., 95, 275–290, 2005.

Martin, J. H.: Glacial-interglacial CO_2 change: The iron hypothesis, Paleoceanography, 5, 1–13, 1990.

Moreno, T., Querol, X., Castillo, S., Alastuey, A., Cuevas, E., Herrmann, L., Mounkaila, M., Elvira, J., and Gibbons, W.: Geochemical variations in aeolian mineral particles from the Sahara-Sahel Dust Corridor, Chemosphere, 65, 261–270, 2006.

Müller, C., Iinuma, Y., Karstensen, J., van Pinxteren, D., Lehmann, S., Gnauk, T., and Herrmann, H.: Seasonal variation of aliphatic amines in marine sub-micrometer particles

at the Cape Verde islands, Atmos. Chem. Phys. Discuss., 9, 14825–14855, 2009, http://www.atmos-chem-phys-discuss.net/9/14825/2009/.

Neusüß, C., Weise, D., Birmili, W., Wex, H., Wiedensohler, A., and Covert, D. S.: Size-segregated chemical, gravimetric and number distribution-derived mass closure of the aerosol in Sagres, Portugal during ACE-2, Tellus B, 52, 169–184, 2000.

Prospero, J. M. and Carlson, T. N.: Saharan Air Outbreaks over the Tropical North-Atlantic, Pure Appl. Geophys., 119, 677–691, 1981.

Prospero, J. M., Glaccum, R. A., and Nees, R. T.: Atmospheric transport of soil dust from Africa to South-America, Nature, 289, 570–572, 1981.

Read, K. A., Mahajan, A. S., Carpenter, L. J., Evans, M. J., Faria, B. V. E., Heard, D. E., Hopkins, J. R., Lee, J. D., Moller, S. J., Lewis, A. C., Mendes, L., McQuaid, J. B., Oetjen, H., Saiz-Lopez, A., Pilling, M. J., and Plane, J. M. C.: Extensive halogen-mediated ozone destruction over the tropical Atlantic Ocean, Nature, 453, 1232–1235, doi:10.1038/nature07035, 2008a.

Read, K. A., Lewis, A. C., Bauguitte, S., Rankin, A. M., Salmon, R. A., Wolff, E. W., Saiz-Lopez, A., Bloss, W. J., Heard, D. E., Lee, J. D., and Plane, J. M. C.: DMS and MSA measurements in the Antarctic Boundary Layer: impact of BrO on MSA production, Atmos. Chem. Phys., 8, 2985–2997, 2008b, http://www.atmos-chem-phys.net/8/2985/2008/.

Rijkenberg, M. J. A., Powell, C. F., Dall'Osto, M., Nielsdottir, M. C., Patey, M. D., Hill, P. G., Baker, A. R., Jickells, T. D., Harrison, R. M., and Achterberg, E. P.: Changes in iron speciation following a Saharan dust event in the tropical North Atlantic Ocean, Mar. Chem., 110, 56–67, 2008.

Schepanski, K., Tegen, I., and Macke, A.: Saharan dust transport and deposition towards the tropical northern Atlantic, Atmos. Chem. Phys., 9, 1173–1189, 2009, http://www.atmos-chem-phys.net/9/1173/2009/.

Schroth, A. W., Crusius, J., Sholkowitz, E. R., and Bostick, B. C.: Iron solubility driven by speciation in dust sources to the ocean, Nature Geosci., 2, 337–340, 2009.

Solmon, F., Chuang, P. Y., Meshkidze, N., and Chen, Y.: Acidic processing of mineral dust iron by anthropogenic compounds over the North Pacific Ocean, J. Geophys. Res., 114, D02305, doi:10.1029/2008JD010417, 2009.

Spokes, L. J. and Jickells, T. D.: Factors controlling the solubility of aerosol trace metals in the atmosphere and on mixing into seawater, Aquat. Geochem., 1, 355–374, 1996.

Turpin, B. J., Saxena, P., and Andrews, E.: Measuring and simulating particulate organics in

the atmosphere: problems and prospects, Atmos. Environ., 34, 2983–3013, 2000.
Washington, R., Todd, M., Middleton, N. J., and Goudie, A. S.: Dust-storm source areas determined by the total ozone monitoring spectrometer and surface observations, Ann. Assoc. Am. Geogr., 93, 297–313, 2003.
Wieprecht, W., Acker, K., Müller, K., Spindler, G., Brüggemann, E., Maenhaut, W., Chi, X., Hitzenberger, R., Bauer, H., and ten Brink, H. M.: INTERCOMP2000: Ionic constitution and comparison of filter and impactor, Atmos. Environ., 38, 6477–6486, 2004.
Yang, G.-P., Zhang, H.-H., Su, L.-P., and Zhou, L.-M.: Biogenic emission of dimethylsulfide (DMS) from the North Yellow sea, China and its contribution to sulfate in aerosol during summer, Atmos. Environ., 43, 2196–2203, 2009.
Zhu, X. R., Prospero, J. M., Millero, F. J., Savoie, D. L., and Brass, G. W.: The solubility of ferric ion in marine mineral aerosol solutions at ambient relative humidities, Mar. Chem., 38, 91–107, 1992.

Table 1. Content of calcium, potassium and iron in impactor samples for two main groups (high dust – low dust) of samples. The percentage in brackets refers to the impactor stage mass.

	Size fraction	Ca $\mu g/m^3$ (%)	K $\mu g/m^3$ (%)	Fe $\mu g/m^3$ (%)
High dust	0.05–0.14	0.004 (1.54)	0.001 (0.31)	0.002 (0.66)
	0.14–0.42	0.006 (0.30)	0.010 (0.51)	0.008 (0.39)
	0.42–1.2	0.080 (1.18)	0.025 (0.37)	0.035 (0.51)
	1.2–3.5	0.527 (2.01)	0.216 (0.82)	0.331 (1.26)
	3.5–10	0.388 (2.05)	0.225 (1.19)	0.305 (1.61)
Low dust	0.05–0.14	0.001 (0.67)	0.000 (0)	0.001 (0.32)
	0.14–0.42	0.002 (0.12)	0.003 (0.19)	0.002 (0.10)
	0.42–1.2	0.017 (1.04)	0.013 (0.80)	0.008 (0.50)
	1.2–3.5	0.056 (0.82)	0.031 (0.44)	0.017 (0.24)
	3.5–10	0.002 (0.04)	0.001 (0.02)	0.002 (0.04)

ACPD
9, 22739–22771, 2009

Table 2. Mean concentration of dicarboxylic acids and MSA detected in impactor samples during the whole campaign by capillary electrophoresis.

	Size fraction μm	Oxalate ng/m^3	Malonate ng/m^3	Succinate ng/m^3	MSA ng/m^3
Organic acids (mean value)	0.05–0.14	0.9	0.1	0.8	0.3
	0.14–0.42	18.6	1.0	1.1	5.0
	0.42–1.2	12.1	1.6	1.6	12.2
	1.2–3.5	14.0	6.0	3.9	11.1
	3.5–10	2.8	2.8	3.8	2.3

ACPD
9, 22739–22771, 2009

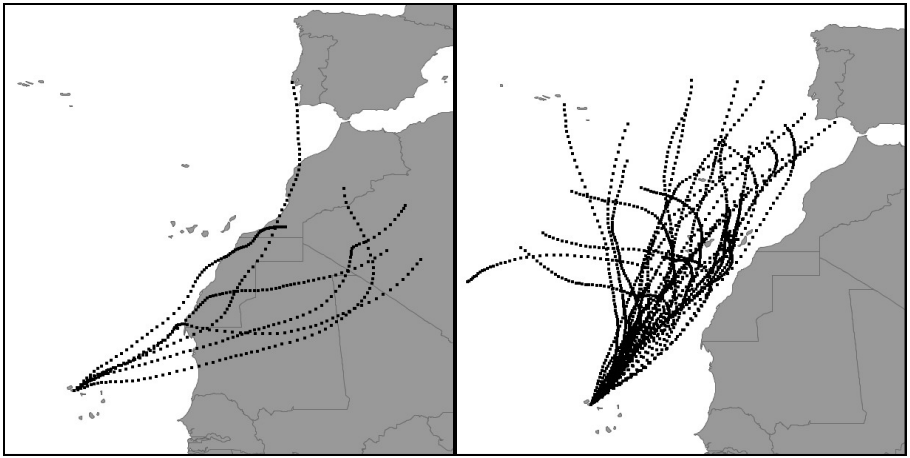

Fig. 1. 72-h back trajectories for the time between 8 and 13 May (left) and 14 May and 14 June (right) starting each at 00:00 UTC in a height of 500 m above ground.

ACPD

9, 22739–22771, 2009

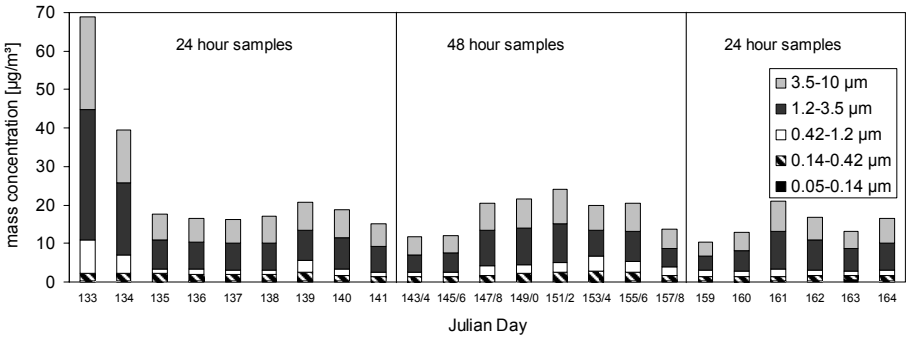

Fig. 2. Mass concentration determined by impactor measurements throughout RHaMBLe intensive.

ACPD
9, 22739–22771, 2009

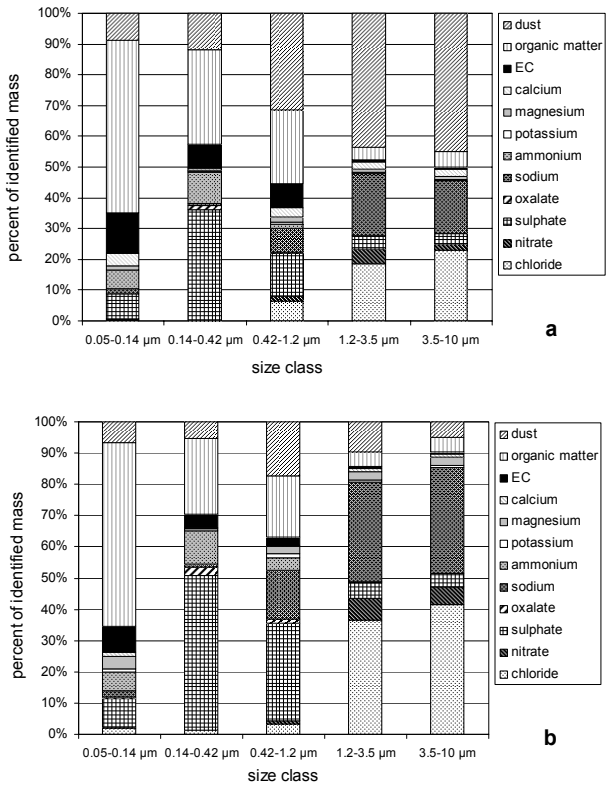

Fig. 3. Identified PM constituents in impactor sample size fractions. **(a)** mean of the two samples collected during dust event, **(b)** mean of the marine influenced period.

ACPD
9, 22739–22771, 2009

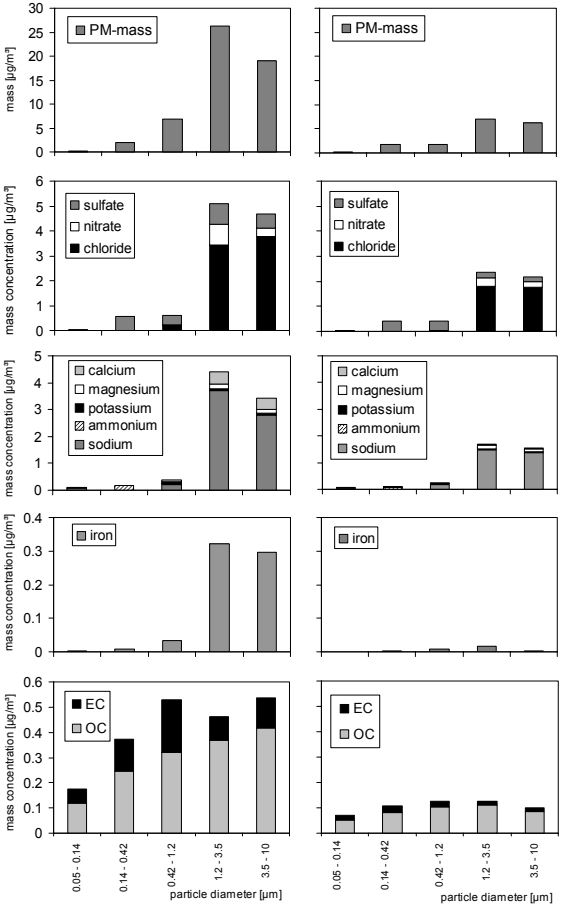

Fig. 4. Detailed size distribution of mass and PM constituents during the dust event (left) and during the low dust marine aerosol (mean values).

ACPD
9, 22739–22771, 2009

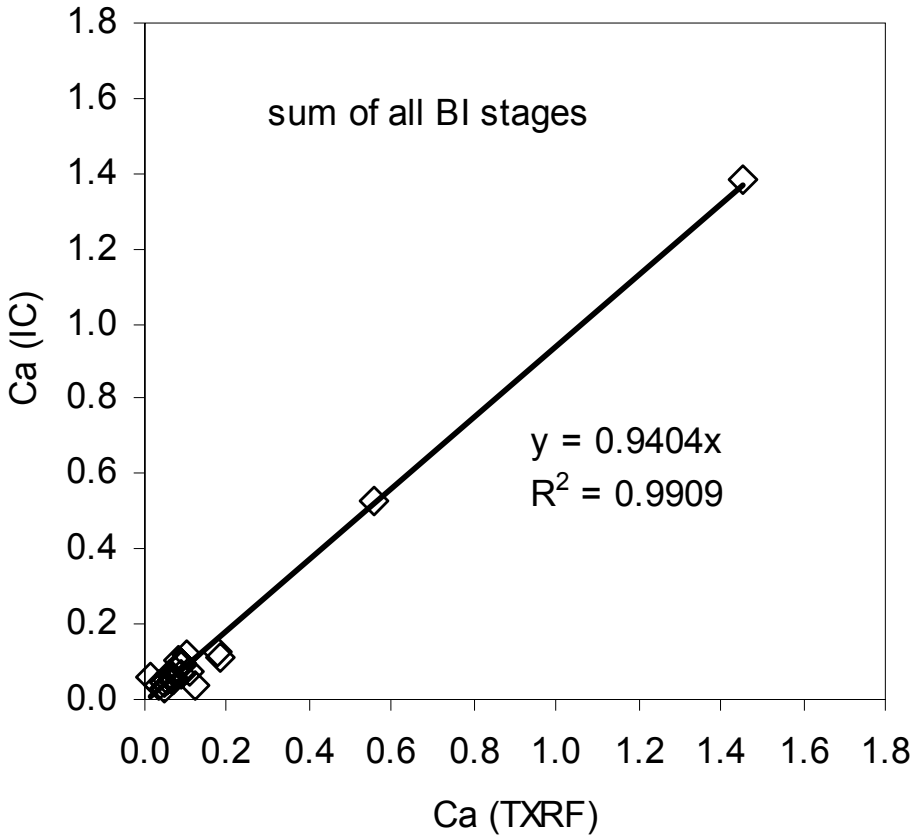

Fig. 5. Correlation of calcium content in impactor samples measured by IC and TXRF.

ACPD
9, 22739–22771, 2009

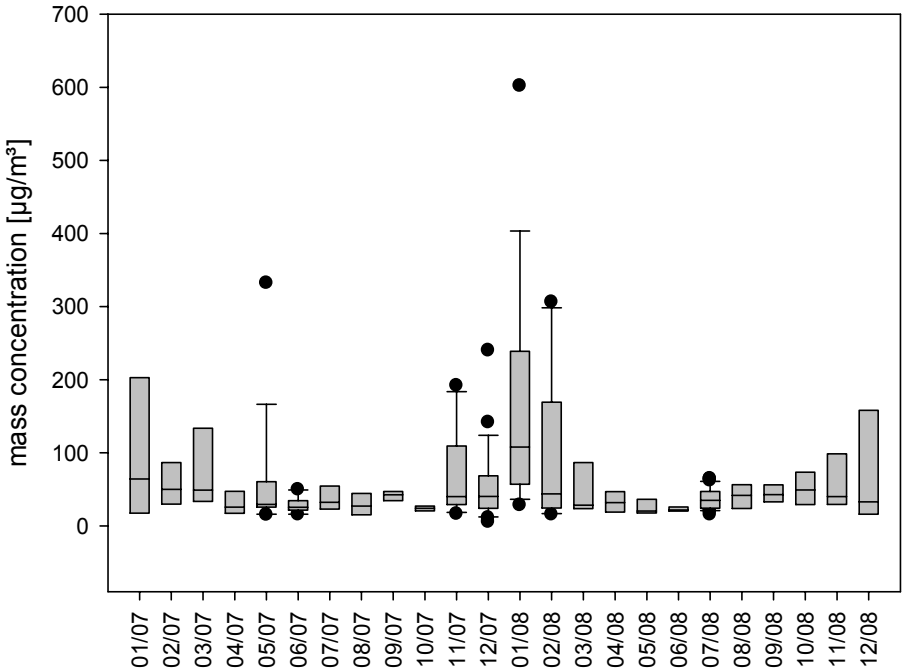

Fig. 6. Box-whisker plot of the monthly measurements of PM mass concentration at the CVAO. Only during intensive campaign the number of monthly measurements is great enough for correct box-whisker presentation.

ACPD
9, 22739–22771, 2009

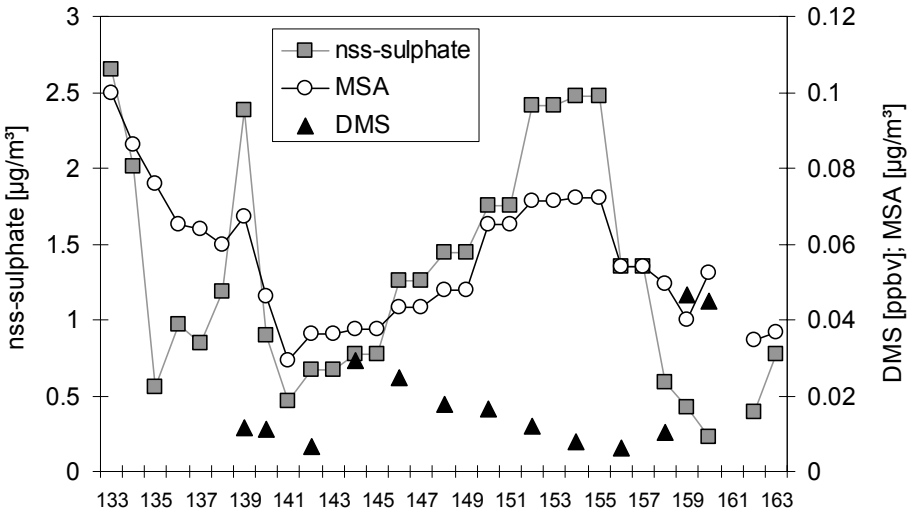

Fig. 7. Concentration of nss-sulphate and methanesulfonic acid (MSA) from filter samples and DMS mean mixing ratios (by courtesy of K. A. Read) during filter sampling intervals.

ACPD
9, 22739–22771, 2009

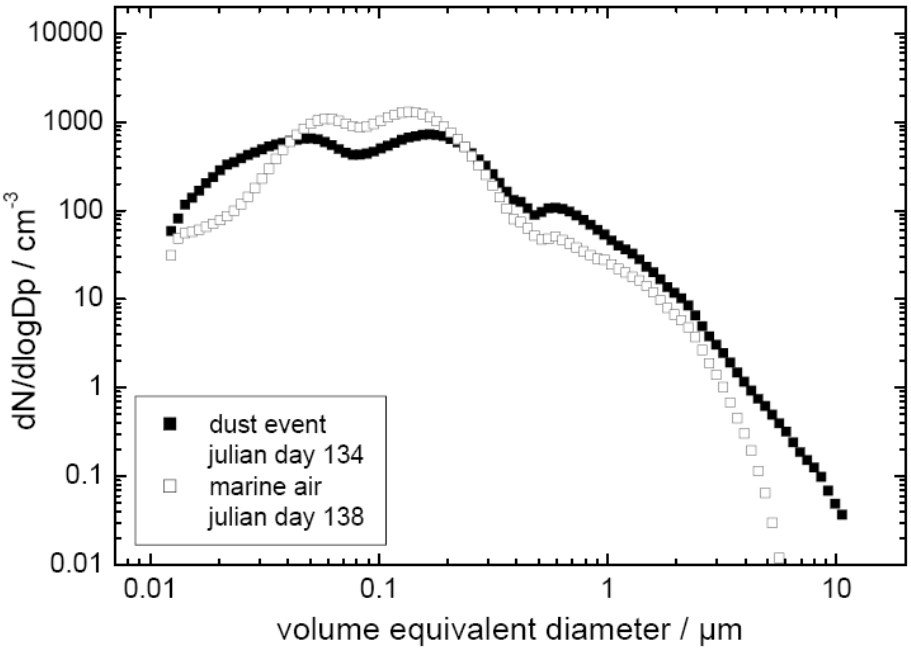

Fig. 8. Particle number size distributions measured at CVAO at 15 May (influenced by Saharan dust) and 19 May (marine air slightly polluted).

ACPD
9, 22739–22771, 2009

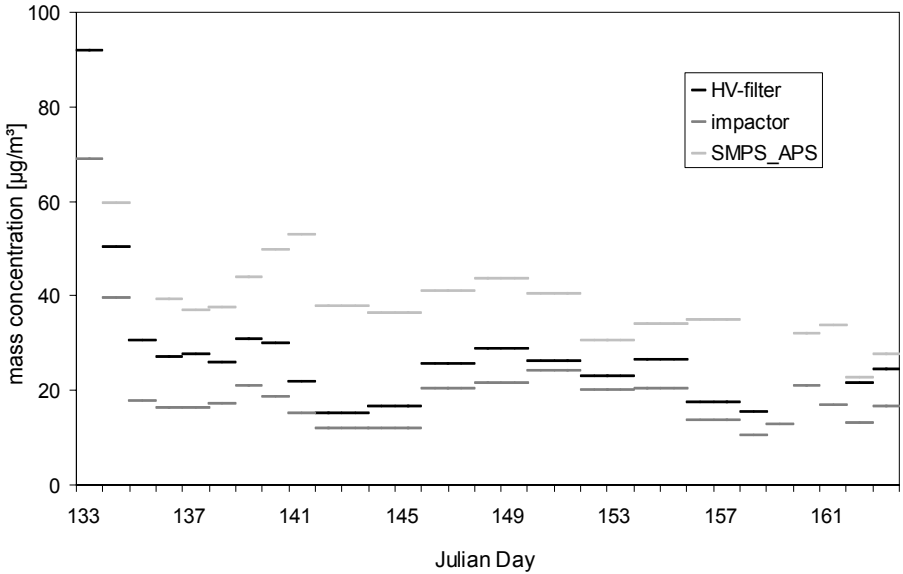

Fig. 9. Comparison of PM mass concentration measured by Digitel HV-filter sampler, five stage Berner low pressure impactor, and APS-SMPS combination.

ACPD
9, 22739–22771, 2009

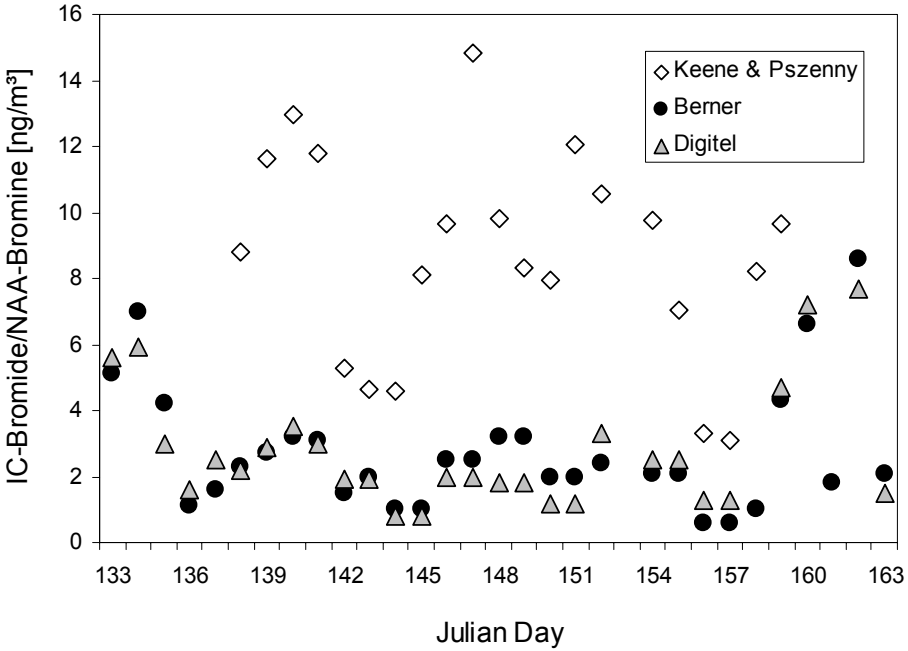

Fig. 10. Comparison of bromide concentrations measured in PM from Digitel HV-filters and Berner impactor samples (sum of all size fractions) with total bromine determination from NAA (by courtesy of A. A. P. Pszenny and W. C. Keene, personal communication, 2009).

ACPD
9, 22739–22771, 2009